ISTITUTO NAZIONALE DI FISICA NUCLEARE

Sezione di Lecce

INFN/TC–97/13
28 Aprile 1997

V. Nassisi, A. Perrone, F.M. De Riccardis, M. Nacucchi, L. Fuggiano:

MEASUREMENT OF Ca, O AND C CONCENTRATIONS IN BONE TISSUES PROCESSED BY LASER IRRADIATION

PACS N.: 42.55.G; 87.50.E; 61.10

SIS–Pubblicazioni
dei Laboratori Nazionali di Frascati

INFN – Istituto Nazionale di Fisica Nucleare
Sezione di Lecce

INFN/TC–97/13
28 Aprile 1997

MEASUREMENT OF Ca, O AND C CONCENTRATIONS IN BONE TISSUES PROCESSED BY LASER IRRADIATION

V. Nassisi[+] and A. Perrone
University of Lecce, Department of Physics, I.N.F.N., 73100 Lecce-I

F.M. De Riccardis and M. Nacucchi
Pastis, C.N.R.S.M., Brindisi-I

L. Fuggiano
Hospital of Lecce " V. Fazzi" 73100 Lecce-I

Abstract

Experimental results of CO_2 and XeCl pulsed laser irradiation on bone tissues are reported. The morphology and composition of the irradiated samples were investigated by an electron microscope and a microanalyser. Different damage of the tissues were obtained utilising the carbon dioxide or excimer lasers. In the irradiated zones by CO_2 laser the C concentration decreased, while the O concentration increased and the Ca concentration decreased only in correspondence of the damaged cut edge. The damaged cut edge resulted to be 180 μm thick. These changes are not marked in the bone irradiated by XeCl laser and the damaged cut edge was only 22 μm thick. This property can be used to shape bone tissues in order to set up small prosthesis.

[+]E-Mail: Nassisi@le.infn.it

1. Introduction

Powerful lasers are used in photodecomposition processes also in orthopedy[1], ophthalmology[2] and dentistry[3]. Hard tissues can change morphologically and chemically after ablation by CO_2 and excimer laser irradiation. During these irradiations different processes are responsible for the bone material ablation which mainly depend on laser wavelength, repetition rate and deposited energy.

The infrared wavelength generated by CO_2 laser is near to the absorption region of water and therefore it can easily interact with any material having a sufficiently high water concentration[4, 5]. Generally, these lasers are applied in photohyperthermia, photocarboniozation and photocoagulation[6].

Excimer lasers are powerful UV light generators and due to their short wavelength they can be efficiently used to heat solid targets at power density lower than those of lasers having wavelengths in the infrared and visible region[7]. Their laser beams can interact with tissues containing proteins, melanin or haemoglobin owing to their UV and visible absorption bands. They are also used for photoablation processes by fast explosion and for photodisruption processes[8, 9].

During laser irradiations the balance between the time necessary for heat conduction and the time between two following laser pulses, brings to different laser tissue interactions even when the same energy density is applied. Moreover, laser irradiation can cause different modifications in irradiated samples. Generally, when an intense laser beam strikes a metal target, a dense hot plasma is obtained at the target surface after a few nanoseconds[10]. For hard tissue samples, the plasma is formed after a few microseconds from onset time of the laser pulse[11] and when the frequency of the plasma matches the laser frequency, the laser beam can not penetrate any further into the plasma. The direct coupling of the laser light with the sample is then stopped[10] and the energy transfer is, however, still possible via electronic heat conducting.

The short excimer wavelengths allow also to process small areas by utilising short focal length lenses. In fact, the basic equation governing the resolution of the minimum resolvable feature size R for a laser beam of good optical quality is [12]

$$R = k\frac{\lambda}{2NA} \qquad (1)$$

where λ is the laser wavelength, k is a constant of proportionality and NA is the numerical aperture of the imaging lens. This property can be used to shape the bone tissue in order to set up small prosthesis.

In this work, we report on the experimental results of processed bones by two different lasers under an equal total energy density deposition: a pulsed CO_2 laser and a pulsed XeCl excimer laser. Because the bones are multicomponent materials composed approximately of 13% water, 27% collagen and 60% hydroxyiapatite and calcium phosphate, it is interesting to study the variations of the main elements: C, O, and Ca. So, we measured the concentration values of the above three elements near the processed bone zones. The C and Ca concentrations indicated the strength of the combustion process caused by the laser irradiation and gave the modification of the organic substances. The O concentration indicated the influence of the atmosphere during the process.

2. Experimental apparatus

Figure 1 shows the experimental setup used in this experiment. The CO_2 laser used was a commercial 300 Hz repetition rate laser. During the experiment its wavelength was 10.6 μm, the energy was 60 mJ contained in about 100 ns, and its spot dimension on the target was 2.3 mm in diameter. The excimer laser was a home-made compact XeCl operating at 308 nm and described in a previous paper [13]. Its output beam had a rectangular cross section of 2x1 cm^2 and its divergence was 3.5 mrad when a cavity with external plane parallel mirrors was applied. During the experiments a 30 cm focal length lens was used to focus the excimer laser beam obtaining a laser spot on the sample of about 1.5 x 0.5 mm^2. The energy per pulse and the repetition rate were fixed at 60 mJ and 1 Hz. The pulse duration was about 20 ns.

During the irradiation the sample were fixed on a holder. Cuts of about 0.5-0.6 mm deep were reached after 10 s for the CO_2 laser (3000 shots) and after 10 min for the XeCl laser (600 shots). Under these conditions the irradiated zones were exposed to the same total energy per cm^2.

3. Diagnostic methods

The investigations were performed by a scanning electron microscope (SEM), PHILIPS XL40 LaB_6 and by an electron probe microanalyser (EPMA), CAMECA SX50.

The SEM allows us to obtain topographical and chemical phase contrast images by scanning the incident electron beam over the specimen surface and detecting the primary electrons backscattered from the interaction between the electron beam and the material.

The detector used was composed of two semicircular solid state diodes fixed above the sample, which were able to collect the electrons emerging from the sample surface along different directions. If the detector signals are summed, the contrast obtained is sensitive to the variation of atomic number of the sample points subjected to the electron bombardment because the backscattering yield depends on the sample mass density. When the signal of one detector is subtracted from that of the other one, the contrast obtained is sensitive mainly to the surface topography because the collection probability of a backscattered electron depends on the relative orientation of the local sample surface with respect to the detectors and in this case topographic contrast images are obtained.

The EPMA allows us qualitative and quantitative determination of the elements present in the sample by analysing the characteristic X-ray emitted from a small volume (approximately a hemisphere of 2 μm radius) of the surface during the electron bombardment.

For these experiments we used a piece of bovine leg, femur, dried for 48 hours and cut into small specimens. All samples processed and coated with a thin gold layer were observed by SEM in order to investigate the morphology of the laser treated regions. Furthermore, some selected samples were included in cold epoxy resin to perform qualitative and quantitative compositional X-ray microanalysis by EPMA. The resin inclusion was performed in two steps: resin filtration (for one week at room temperature) and subsequent polymerisation (for few hours). Then the samples were cut and subjected to a conductive coating and analysed in cross section.

4. Results and discussion

All irradiated samples were analysed by using the SEM at low magnification (≈ 400x) in order to extend the field of view to the entire treated region.

After the XeCl irradiation, the samples were examined with the naked eye and no damaged edges were observed. On the contrary, the samples irradiated with the CO_2 laser became flake.

Figure 2 shows the backscattered electrons (BSE) image, obtained in topographic contrast mode, of the irradiated zone by 3000 CO_2 laser pulses. The irradiated zone was an hole which edges were smooth because of the strong vaporisation action. This action influenced the cut edges which did not become very shape. The presence of bubbles around the hole indicates a strong local increase of the temperature. In Fig. 3 a BSE image of the same region obtained by using the chemical contrast mode is illustrated. Different contrast zones can be observed. The finding indicated a variation of the bone composition in the laser treated region. The treat areas presented flakes and fractures due to the relatively high temperature reached during the irradiation.

Figure 4 shows a BSE image of the cut generated by XeCl laser irradiation obtained using the topographic contrast mode. The cut wall seemed smooth and its edges were very shape due to the photoablation process and to the fast explosion during laser irradiation. It is worth to note that its bottom was flat. In Fig. 5 a BSE image of the same region but in chemical contrast mode is showed. It was not possible to distinguish any heat affected zone surrounding the cut. The bone layers did not flake as in the CO_2 laser cut (see Fig.3). This last result could not be ascribed to the small repetition rate of the XeCl laser used. In fact, investigations performed with a poor divergence commercial XeCl laser at repetition rate in excess of 50 Hz and with the same total energy density became only black but not flake.

The compositional analysis was performed by using the EPMA on a cross section of the samples included in resin. The sample cross sections are shown in Figs. 6 and 7 related to the processing with the CO_2 and with the XeCl laser, respectively. The electron beam impinges normally to the sample cross section. The goal of the analysis was to measure the variation in the bone composition along a line from the non irradiated zone (inside) to the irradiated one (external).

For all samples, the acquisition of calibration data for C, O, and Ca was performed as ratio of the concentration measured in irradiated zones with respect to the concentration measured in zones very far from those processed. In particular, for each sample, the X-ray intensities of C Kα, O Kα, and Ca Kα emitted lines from processed zones were divided from the corresponding X ray intensities from zones non-processed of the same bone. The values are called k ratios and they represent, at the first order approximation, the normalised concentrations of C, O, and Ca. Further, no matrix correction was applied to the k ratios because these mathematical procedures are not valid for porous material; anyway the matrix effect in the k ratio numerator compensated that of denominator because both, numerator and denominator, referred to signals emitted from the same bone. In these measurements an electron beam of 10 keV having a current of 30 nA was chosen in order to increase the signal to noise ratio.

Figure 8 reports the k ratios of C, O, and Ca as a function of the distance along the line starting from the internal part of the bone to the external one around the hole, for the bone processed with the CO_2 laser. The distance between two successive analysed points was about 36 μm; the total path length was approximately 0.5 mm. The line scan was repeated four times in order to take into account the statistical noise; the total number of measurements was 60 and its corresponding acquisition time was 65 minutes. The three elements analysed presented a strong variable concentration for a depth of about 180 μm (damaged cut edge) indicating that the irradiation modified the composition of the bone. Indeed, in more external part the concentration varied slight but the measured values did not correspond to those of the resin where we expected an high carbon concentration and a very low concentration of oxygen and calcium (≈ 0). The normalised carbon content varied from $0.8 \div 0.9$ in the internal part to $1.6 \div 1.7$ in the external one. The low carbon concentration measured in the internal part could be ascribed to the carbon oxidation process with the oxygen contained in the atmosphere. In fact, in this zone, the concentration of the O increased by about 20 %. The increase of the oxygen concentration could have favoured the oxidation of the carbon to CO and CO_2 gas. This last evaporating impoverished the bone of C element. The Ca concentration seemed to be 1 into the bone. Indeed, it was very surprising the no zero concentration of Ca, as well as O, in the external part. This analysis was limited by our scanning line which did not reach the zone having pure resin due to the very extensive thermal damage cut edge. Usually, the carbon concentration into the resin is about 8

times higher than that in a normal bone. This value was obtained in the measurements performed with the XeCl laser. Therefore, in the CO_2 processed bone, the concentration values measured in the external part were influenced by the presence of the resin penetrated in the flaked zones; in fact, the Ca percentage did not reach the zero value. At the 500 μm distance, the Ca concentration decreased up to 0.8 indicating that this region, with a minor calcium concentration, was a thermal damage zone.

Figure 9 reports the k ratios of C, O and Ca as a function of the distance along the line across the cut edge for the bone processed with the XeCl laser. The distance between two successive analysed points was about 11 μm; the total path length was approximately 75 μm. The k value for each point is an average over eight measurements. The total number of measurements was 64 and its corresponding acquisition time was 75 minutes. The sixth point is a transition one from the bone to the resin (see the sharp cut in Fig. 7). The epoxy resin was rich in carbon but poor in oxygen and did not contain calcium. In this case, the C percentance was 1 inside the bone until the 42 μm distance, and it became 8 after 64 μm. The Ca concentration remained constant to 1 inside the bone and became zero just after the transition zone estimated 22 μm thickness (Fig. 9). Note that the cut was very shape indicating a small damaged cut edge. This result was consistent with our previous SEM observations.

5. Conclusions

Cuts on the bone tissues were performed with two different lasers and analysed after an equal energy density deposition. SEM observations and X-ray microanalyses lead to the following conclusions:

1) the cut made by the XeC1 laser had shape edges and a flat bottom due to the laser photoablation action; in contrast, the cut made, with the same energy density, by the CO_2 laser showed thermal damage with fractures and bubbles and an extensive transition zone from the bone to resin wider than 500 μm.

2) the analysis of the C, O, and Ca concentrations revealed a high content of carbon in the irradiated zone with CO_2 laser due to resin penetration in the flaked zones. In fact, these samples had very flaked zones and fractures due to the relatively high temperature

reached during the irradiation. These changes were not present in the bone irradiated by the XeCl laser.

In spite of the good cut quality and the low contamination of the elements in the sample irradiated with the XeCl laser, this method is not yet applicable due to the long time necessary to realise cuts in the bones.

5. References

1. Abelow S.P. Use of laser in orthopedic surgery. *Othopedics.* 1993: 16:5; 551-556

2. Gibson K.F., Kernohan W.G. Laser in medicine-a review. *J. of medical Engineering & Technology* 1993: 17; 51-57

3. Goldman L., Goldman B. and Van Lieu N. Current laser dentistry. *Laser and Medicine*, 1987: 6; 559-562

4. Frenz M., Zweig A.D., Romano V. and Weber H.P. Laser tissue interation. *Proc. SPIE,* 1990: 1202; 22-33

5. Forrer M., Frenz M., Romano V., Altermat H.J., Weber H.P., Silenok A., Istomyn M. and Konov V.I. Bone-ablation mechanism using CO_2 lasers of different pulse duration and wavelength. *Appl. Phys. B* 1993: 56; 104-112

G.I.

6. Zhelton G.I., Podoltsev A.S., Kirkovsky A.I., Belokon M.V., Glazov V.N.and Linnik L.A. Applying the mixture of fundamental relation and the second armonic of a neodymium laser for therapeutic and photocoaculation of eyeground tissues. *Bullettin of the Russian Academy of Sciences Physics.* 1996: 59; 1003-1007

7. Luches A., Martino M., Nassisi V. and Pecoraro A. Generation of self-pulsed multiply charged ions by an XeCl excimer laser. *Nucl. Instr. Method.* 1992: A322; 166-169

8. Wolgin M. et al. Excimer ablation of human intervertrebal disc at 308 nm. *Laser in surg. and medicine.* 1989: 9; 124-131

9. Sviridov A.P. et al. Excimer laser drilling of bone. Shockwave and profile measurements. *Proc. SPIE* 1995: 2323; 234-249

10. Irons F.E. and Peacock N.J. A spectroscopic study of the recombination of C^{6+} to C^{5+} in an expanding laser-produced plasma. *J. Phys. B* 1974: 7; 2084-2099

11. Teng P., Nishioka N.S., Anderson R.R. and Deutsch T.F. Optical studies of pulsed-laser fragmentation of biliari calculi. *Appl. Phys B* 1987: 42; 73-78

12. Znotins T.A. Excimer lasers in microlithography. *Laser & Optronic* 1988: May; 55-61

13. Luches A., Nassisi V. and Perrone M.R. Output characteristics of an excimer laser with delayed double preionisation. *J. Phys. E: Sci. Intrum.* 1987: 20; 1015-1018

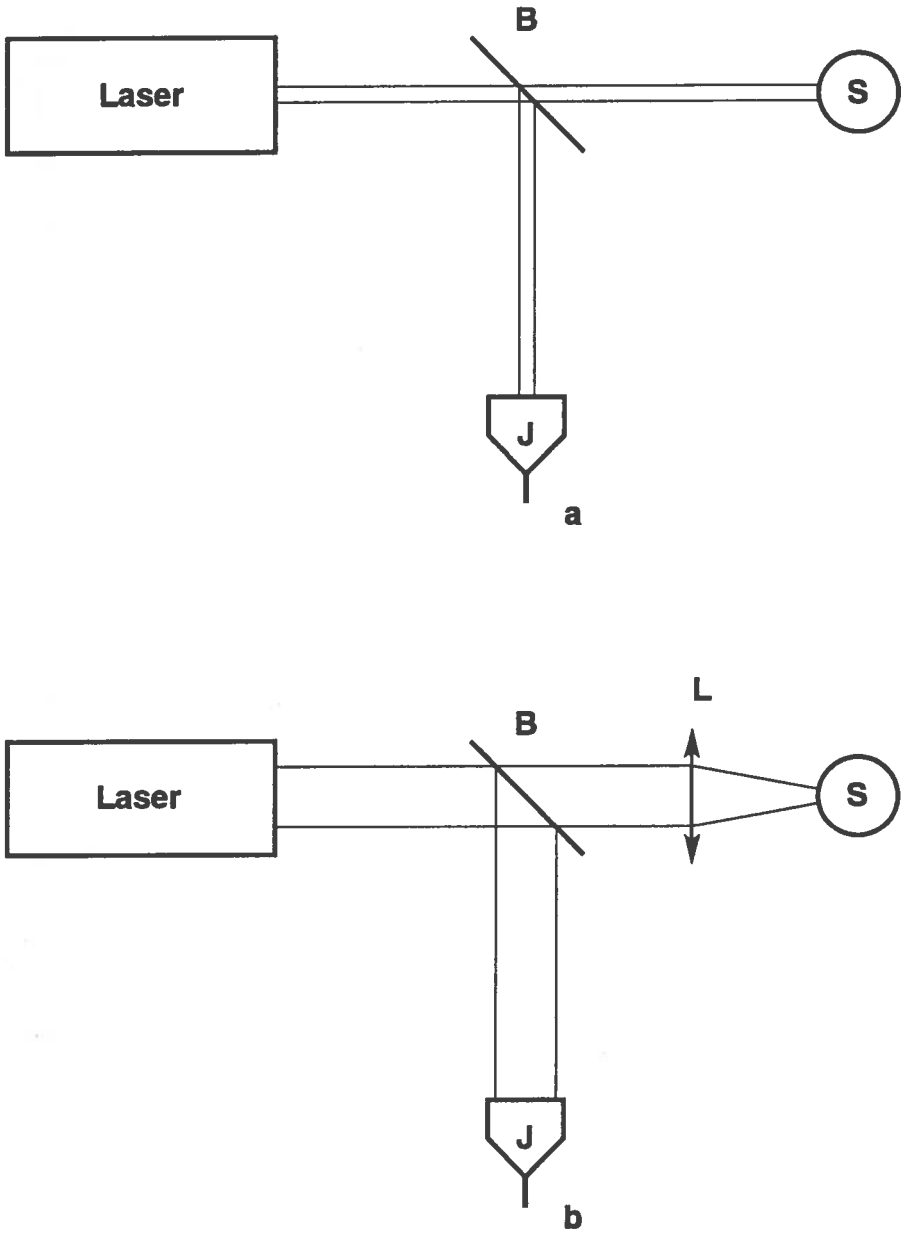

Fig.1: Experimental setup: a) CO_2 laser, S - sample; b) XeCl laser, S - sample, B - beam splitter, J - Joule-meter, L - lens.

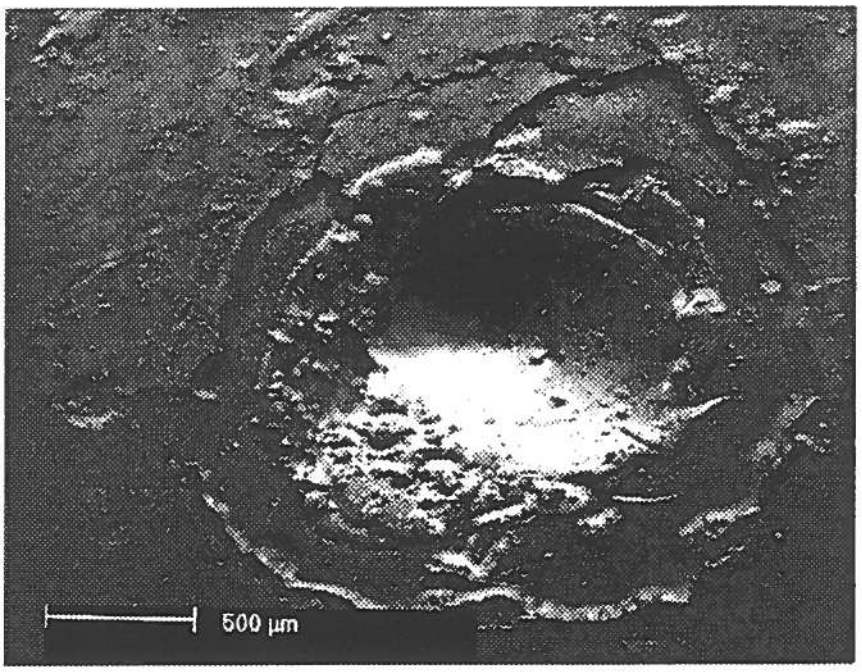

Fig. 2: BSE image in topographic contrast mode of the hole made by the CO_2 laser after 3000 pulses (E_T=60 mJ)

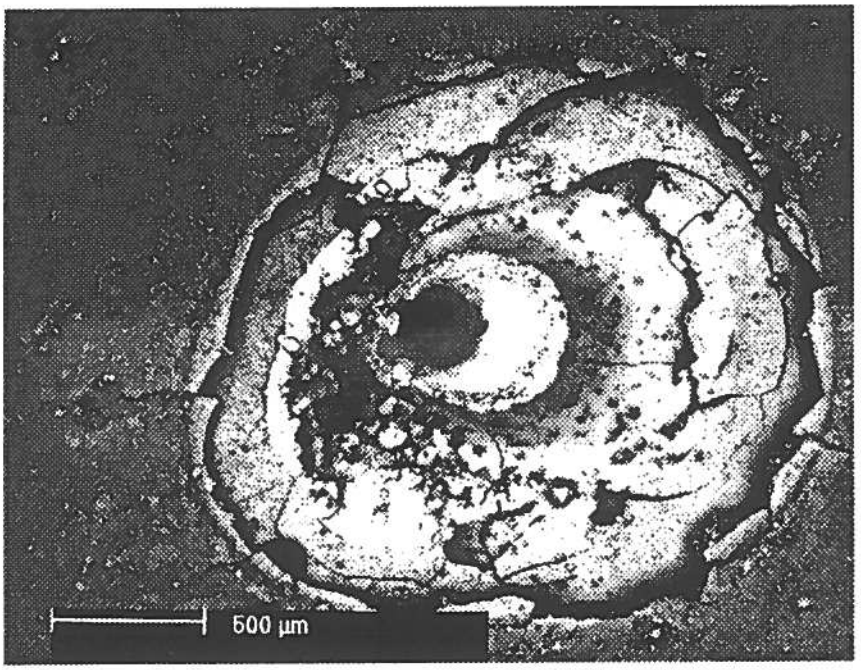

Fig. 3: BSE image in compositional contrast mode for the same sample of Fig.2.

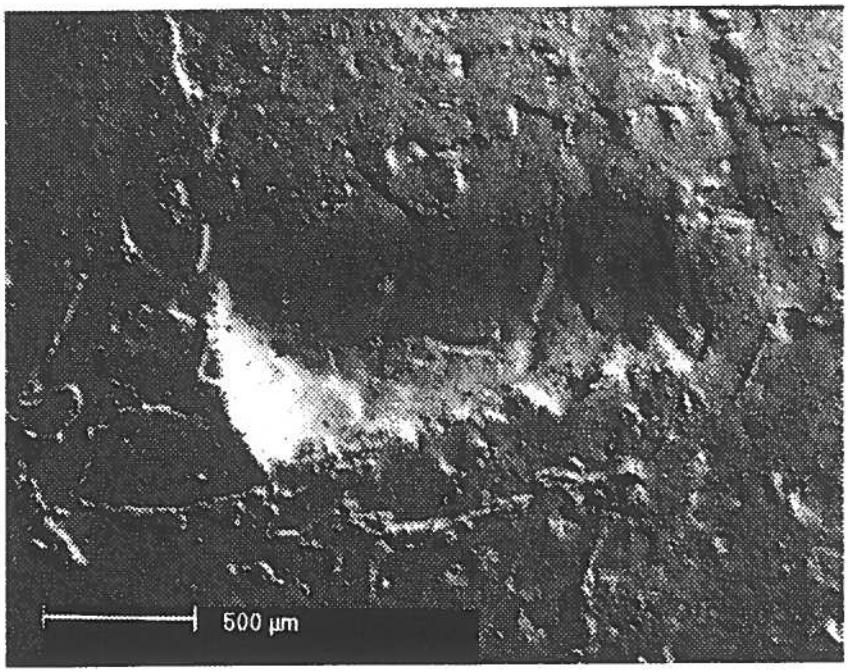

Fig. 4: BSE image in topographic contrast mode of the cut made by the XeCl laser after 600 pulses (E_T=60mJ).

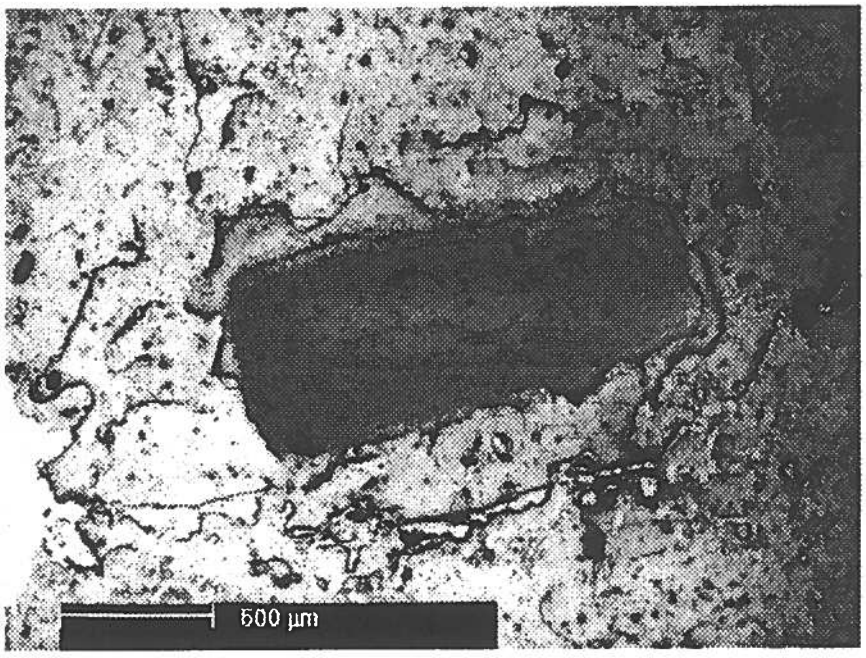

Fig. 5: BSE image in compositional contrast mode for the same sample of Fig. 4.

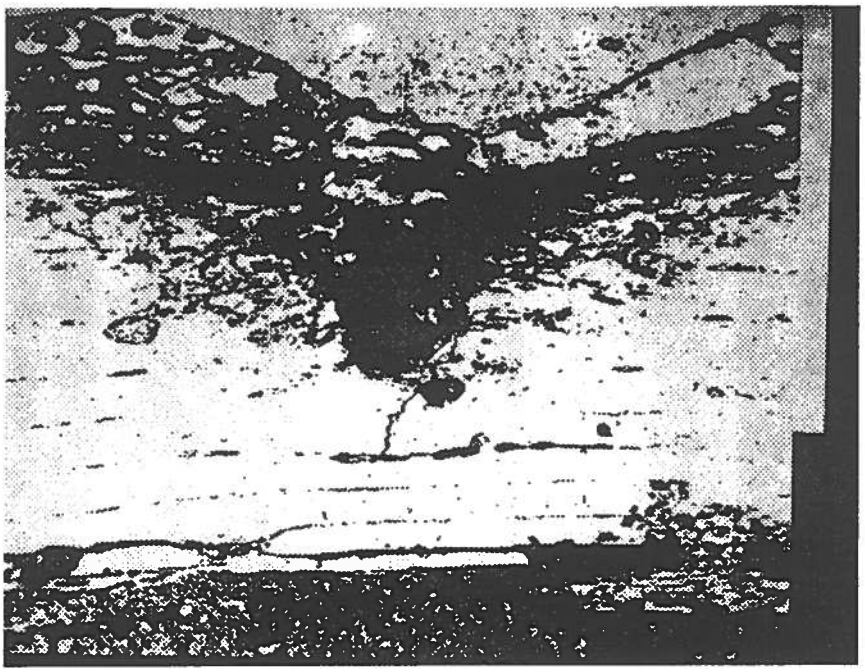

Fig. 6: Scheme of a cross section of the bone treated with CO_2 laser and included in resin.

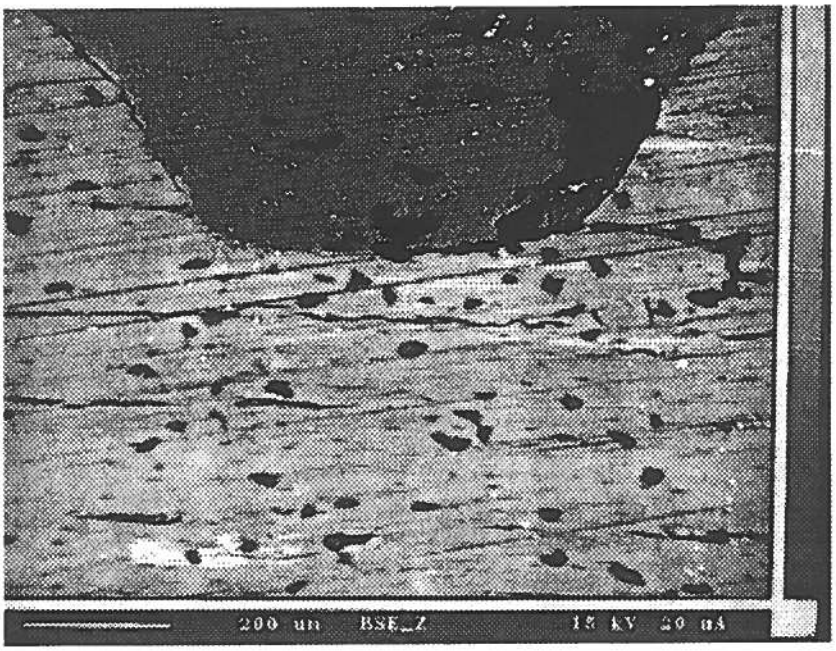

Fig. 7: Scheme of a cross section of the bone treated with the XeCl laser and included in resin.

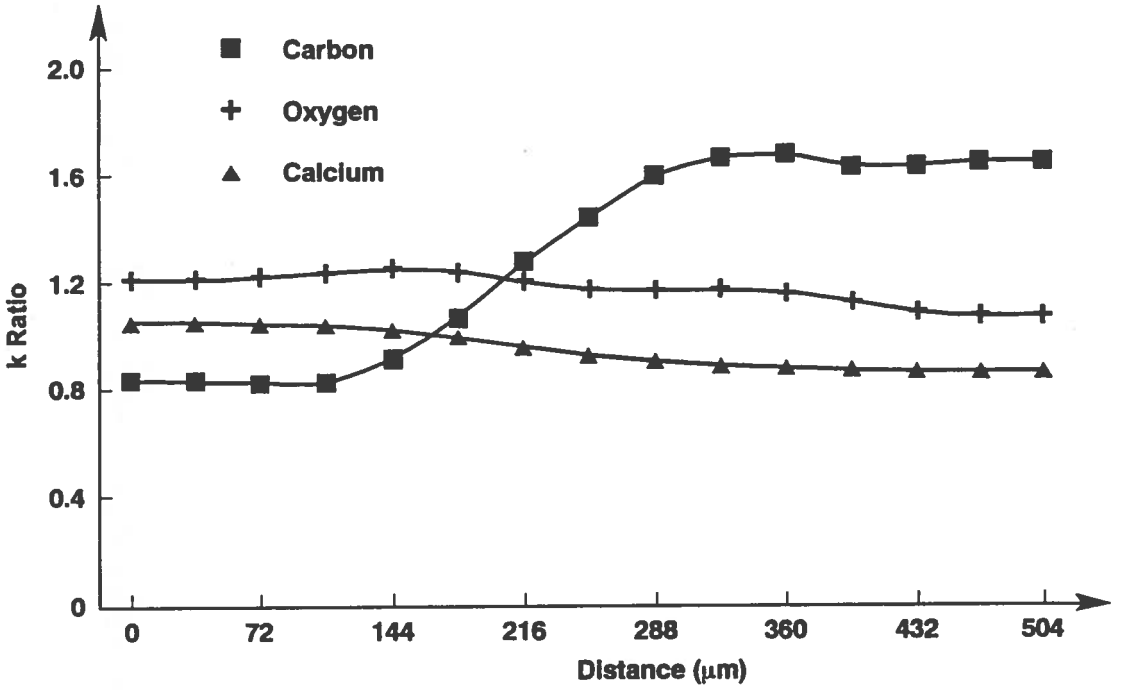

Fig. 8: Carbon, oxygen and calcium concentrations as a function of the distance along the line from the inside of the bone to the damaged zone. Sample processed by 3000 CO_2 laser pulses.

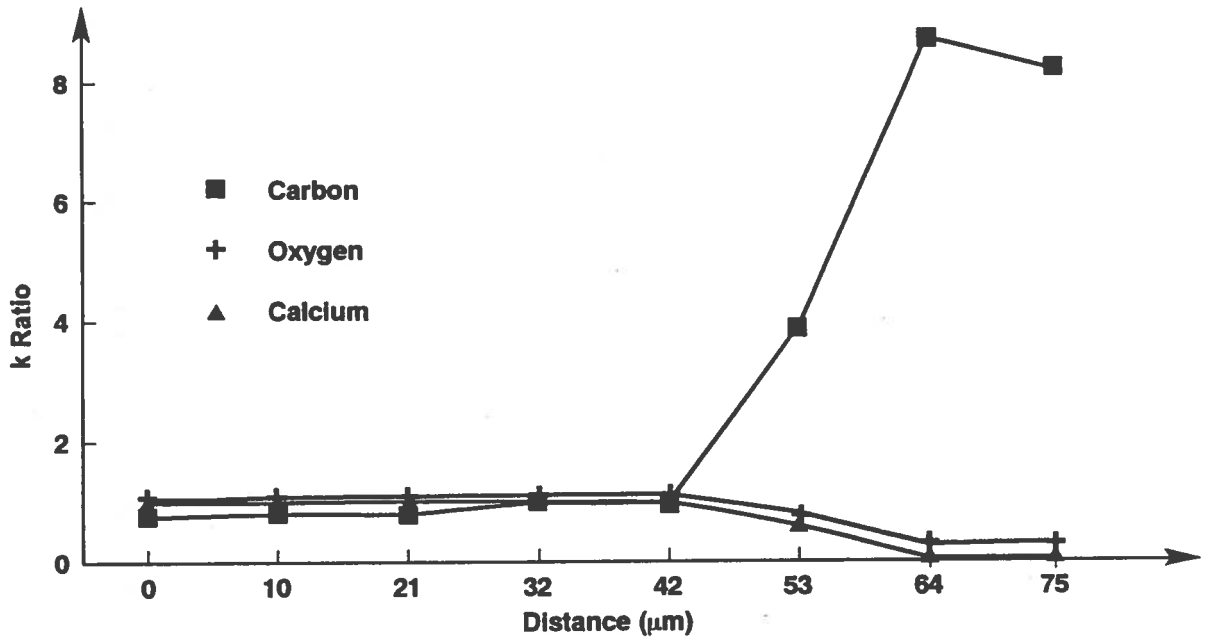

Fig. 9: Carbon, oxygen and calcium concentrations as a function of the distance along the line from the inside of the bone to the damaged zone. Sample processed by 600 XeCl laser pulses.